Electronic Supplementary Material (ESI) for Energy & Environmental Science.
This journal is © The Royal Society of Chemistry 2022

Electronic Supplementary Information

Enabling rapid pseudocapacitive multi-electron reaction by heterostructure engineering of vanadium oxide for high-energy and high-power lithium storage

Feng Su,[ab] Feifei Xing,[ab] Xiao Wang,[a] Fangyan Liu,[a] Liangzhu Zhang[a] and Zhong-Shuai Wu*[ac]

[a] State Key Laboratory of Catalysis, Dalian Institute of Chemical Physics, Chinese Academy of Sciences, 457 Zhongshan Road, Dalian 116023, China.

E-mail: wuzs@dicp.ac.cn

[b] University of Chinese Academy of Sciences, 19 A Yuquan Rd, Shijingshan District, Beijing 100049, China

[c] Dalian National Laboratory for Clean Energy, Chinese Academy of Sciences, 457 Zhongshan Road, Dalian 116023, China

Experimental Section

Materials Preparation

To synthesize 2D V_2O_5/graphene heterostructure, graphene oxide (GO) nanosheets were used as 2D templates to load the V source. GO suspension (2 mg mL^{-1}, 50 mL) was sonicated for 15 min to disperse GO nanosheets. In parallel, 200 mg NH_4VO_3 was dissolved in 15 mL H_2O. The NH_4VO_3 solution was slowly added into the GO suspension under stirring to prevent agglomeration. The mixed dispersion was poured into liquid nitrogen to be quickly frozen. After the removal of ice by freeze-drying, the precursor was obtained. Finally, 180 mg precursor was put into a 50 mL sealed beaker and annealed at 350 °C for 1 h with a heating rate of 2 °C min^{-1} to obtain 2D V_2O_5/graphene heterostructure. For comparison, V_2O_5 cryogel was prepared by sol-gel method.[1] In detail, 1 g commercial V_2O_5 was dissolved in a mixed solution of 50 mL H_2O_2 (30%) and 50 mL H_2O and stirred for 24 h. After aged for 4 days, bilayered V_2O_5 hydrogel was formed and subsequently dried by freeze-drying to obtain V_2O_5 cryogel. Additionally, orthorhombic V_2O_5 was prepared by annealing commercial NH_4VO_3 in air at 350 °C for 5 h.

Materials Characterization

The morphology, composition, and structure of materials were characterized by field emission scanning electron microscopy (JSM-7800F), transition electron microscopy (JEM-2100), atomic force microscopy (Veeco nanoscope multimode II-D), powder X-ray diffraction (Rigaku SmartLab equipped with Cu Kα radiation), Raman spectrometer (Bruker Optics Senterra, 532 nm), X-ray photoelectron spectroscopy (ThermoFisher Escalab 250Xi) and N_2 adsorption/desorption isotherms (Quadrasorb evo).

Electrochemical Measurements

The electrodes were prepared by mixing the active material, Ketjen black and poly(vinylidene fluoride) at a mass ratio of 8:1:1 in N-methyl pyrrolidone solvent to form a uniform slurry, which was then coated on carbon-coated Al foil and dried at 100 °C under vacuum. For half-cell tests, CR2032-type coin cells with Al-coated bottom casing were assembled in an argon-filled glovebox with H_2O and O_2 concentration below 0.5 ppm, using lithium metal as both counter and reference electrodes, glass fiber separator (Whatman GF/D). A concentrated ether-based electrolyte composed of 4 M lithium bis-(fluorosulfonyl)imide (LiFSI) dissolved in 1 L 1,2-dimethoxyethane was used to alleviate the dissolution of vanadium oxide in the electrolyte. In addition, the low viscosity of ether solvent and high solubility and dissociation constant of LiFSI salt promise superior ionic conductivity of the concentrated ether-based electrolyte, which is a key parameter for achieving high rate performance. To fabricate the symmetric full cells, the V_2O_5/graphene electrodes were prelithiated to 2.45 V *vs.*

Li^+/Li at 0.1 A g^{-1} in half cells, and two prelithiated electrodes with identical mass loading were assembled into CR2032-type full cell. GCD and GITT measurements were performed on a LANHE M340A battery test system. GITT was carried out with a galvanostatic current pulse of 0.1 A g^{-1} for 10 min and a subsequent relaxation time of 1 h. CV test was conducted on an electrochemical workstation (CHI 760E). EIS was measured by CHI 760E in the frequency range of 100 kHz to 0.01 Hz with an amplitude of 5 mV.

DFT calculations

All DFT calculations were performed using the Vienna Ab initio Simulation Package (VASP).[2] The projector augmented-wave pseudopotential method with the Perdew-Burke-Ernzerhof (PBE)[3,4] exchange-correlation functional and a plane-wave cutoff energy of 400 eV was adopted. DFT-D3 method of Grimme with zero-damping function[5,6] was used to calculate the van der Waals correction. DFT+U was used to consider the on-site Coulomb interaction for vanadium 3d states and the value of Ueff (U-J)[7] was set to 3.25 eV. All the structures were fully relaxed until the residual energy in iterative solution of the Kohn-Sham equation and force declined to less than 10-4 eV and 0.03 eV/Å, respectively. The V_2O_5/graphene heterostructure model was composed of a 1×2×1 V_2O_5 layer and a 3×3×1 graphene layer. The perpendicular direction was set to 30 Å with A vacuum layer added to avoid artificial interaction between periodic images. The Brillouin zone integration was performed using a 3×5×1 k-mesh.

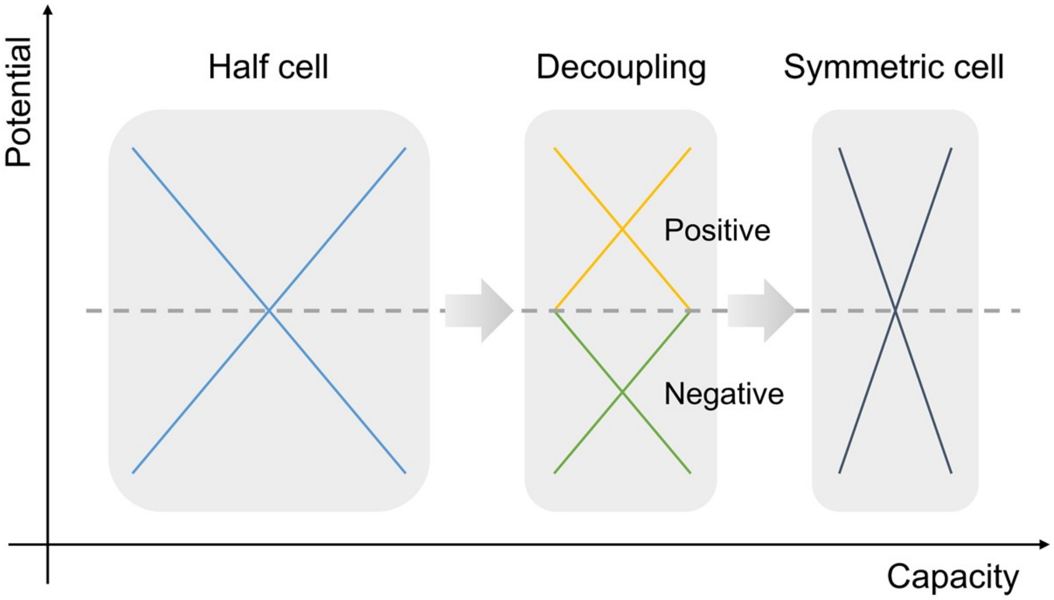

Fig. S1 Schematic illustration of the construction strategy for symmetric cells.

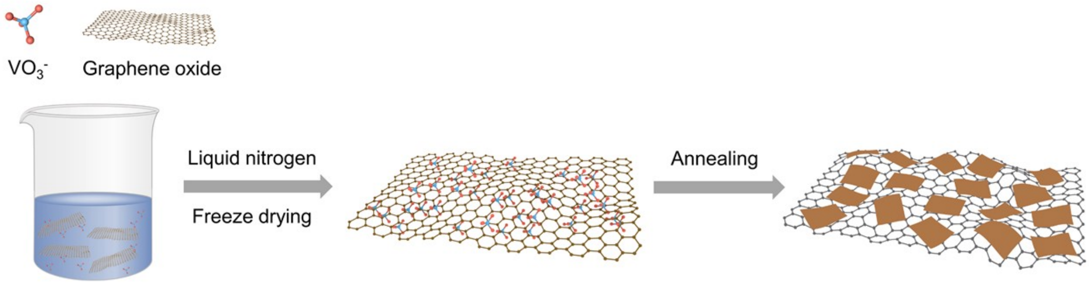

Fig. S2 Schematic illustration of the preparation of 2D V_2O_5/graphene heterostructure.

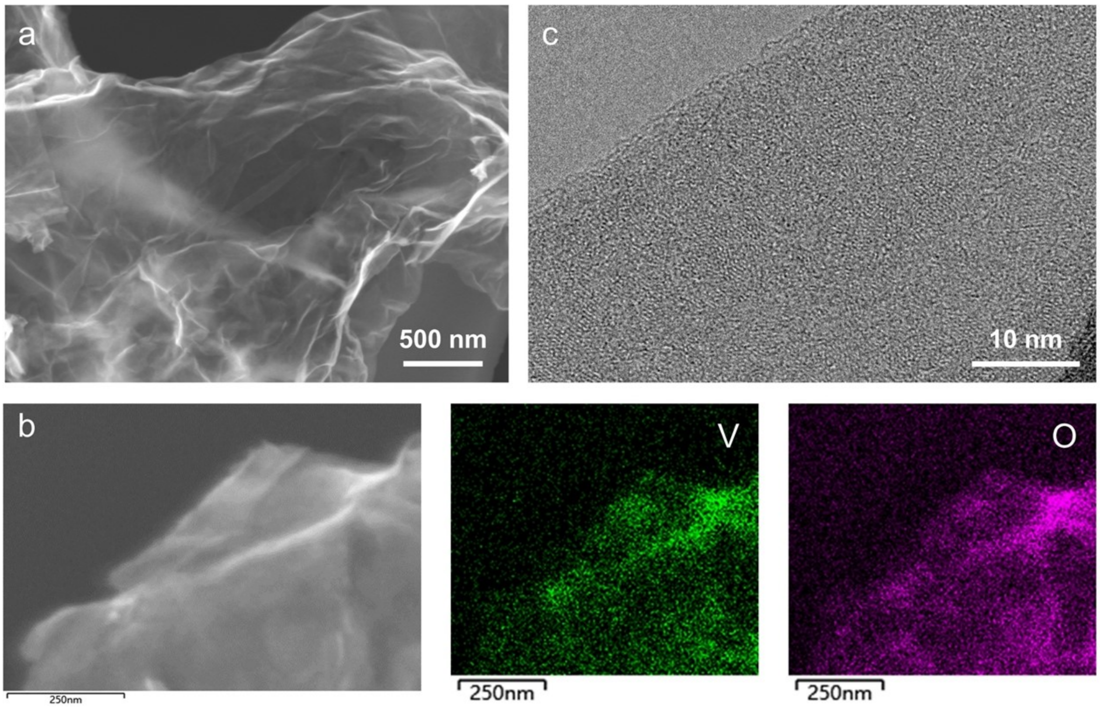

Fig. S3 (a) SEM image, (b) EDS elemental mapping and (c) TEM image of 2D V_2O_5/graphene heterostructure.

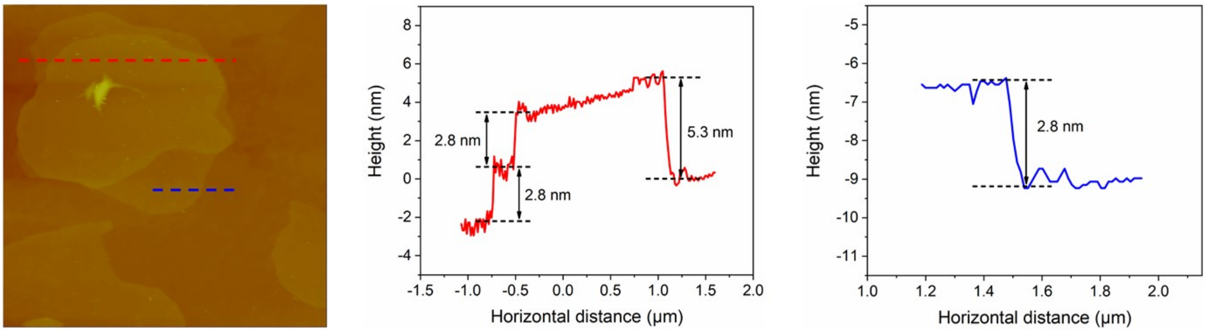

Fig. S4 AFM image and corresponding height profiles of 2D V_2O_5/graphene heterostructure.

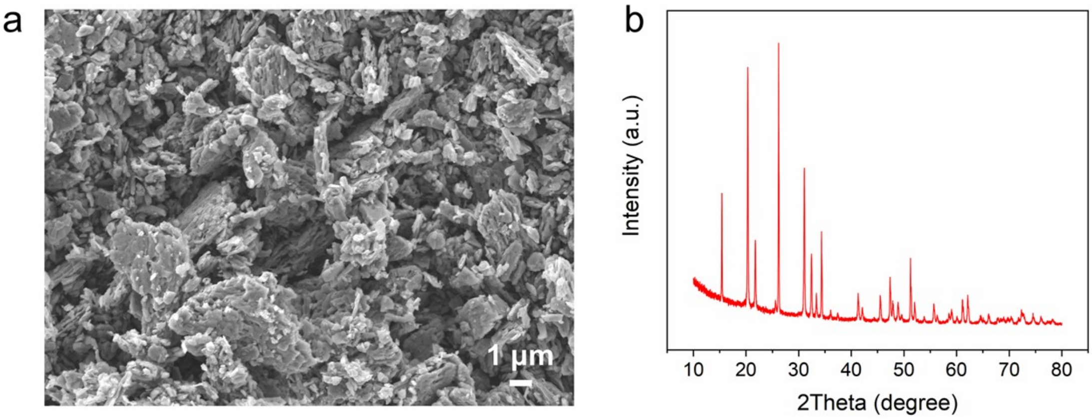

Fig. S5 (a) SEM image and (b) XRD pattern of orthorhombic V_2O_5.

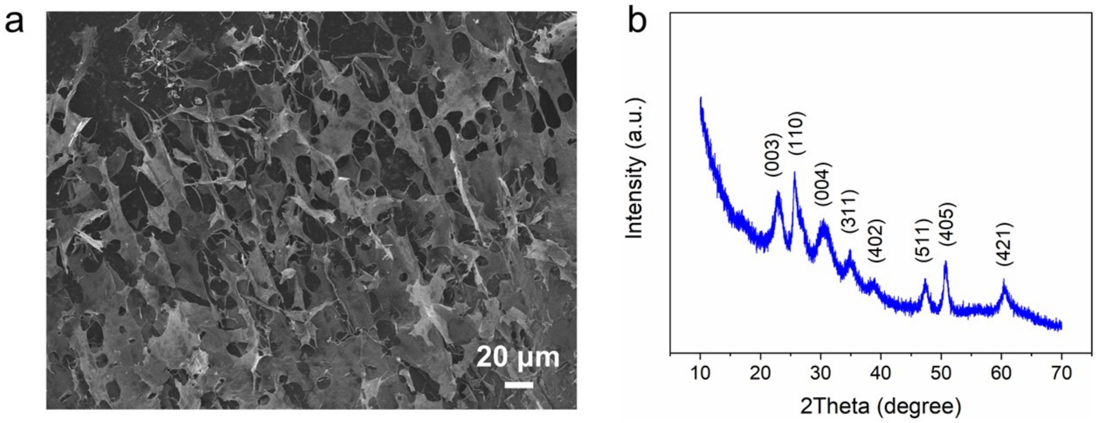

Fig. S6 (a) SEM image and (b) XRD pattern of V_2O_5 cryogel.

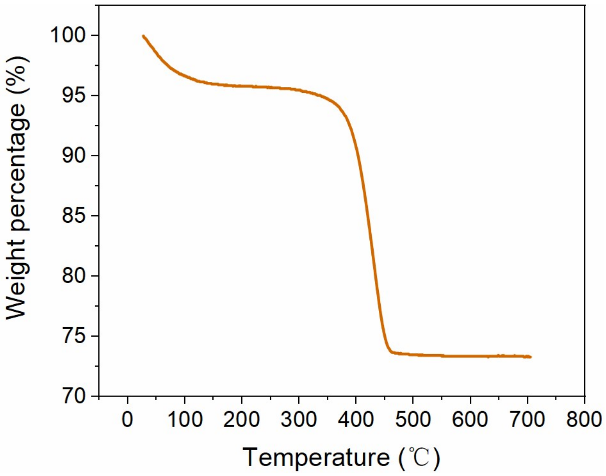

Fig. S7 TGA curve of 2D V_2O_5/graphene heterostructure.

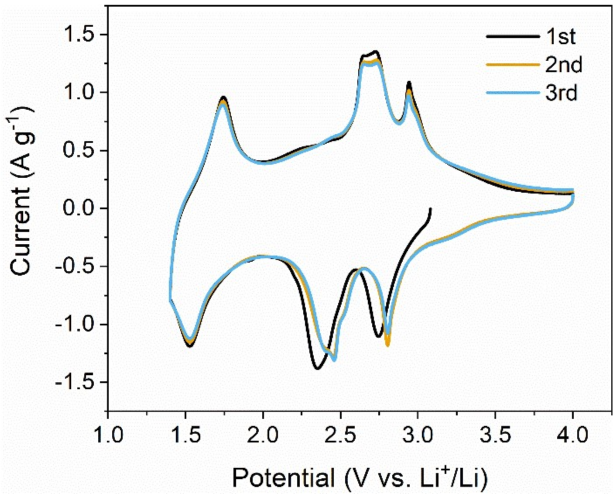

Fig. S8 CV curves of the initial three cycles of 2D V_2O_5/graphene heterostructure at 1 mV s^{-1}.

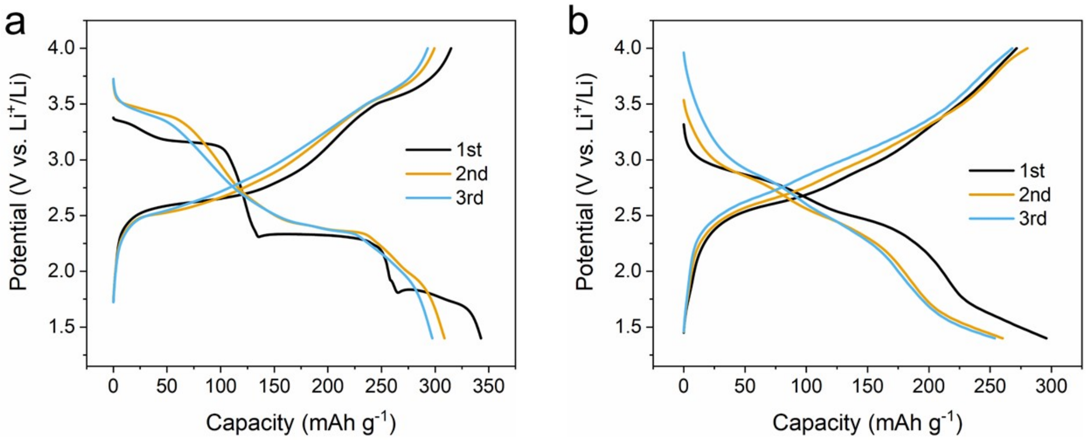

Fig. S9 GCD profiles of the initial three cycles for (a) orthorhombic V_2O_5 at 1 C and (b) V_2O_5 cryogel at 0.1 C.

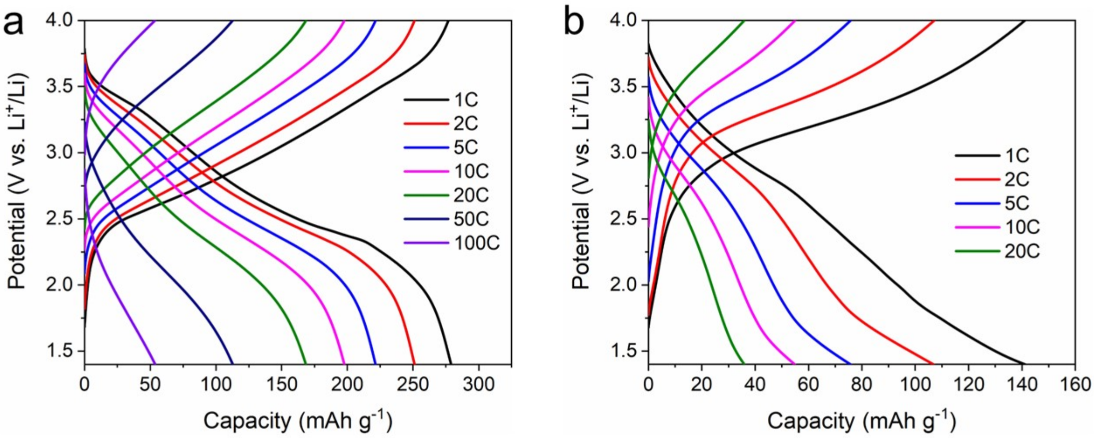

Fig. S10 GCD profiles at different current rates of (a) orthorhombic V_2O_5 and (b) V_2O_5 cryogel.

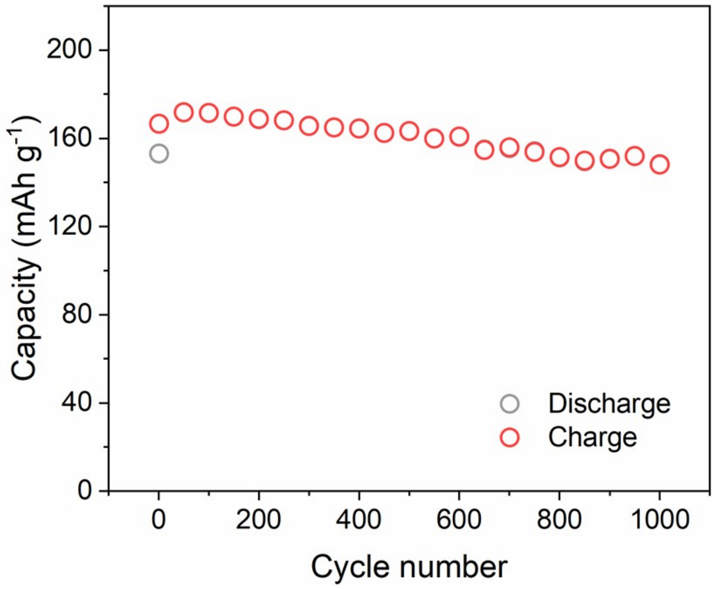

Fig. S11 Cycling performance of 2D V_2O_5/graphene heterostructure at a current rate of 100 C.

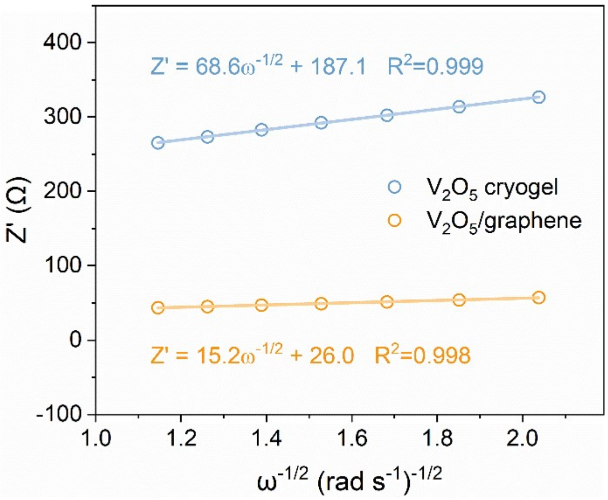

Fig. S12 Linear relationship between real part of impedance (Z) and frequency$^{-1/2}$ ($\omega^{-1/2}$).

The diffusion coefficients of 2D V_2O_5/graphene heterostructure and V_2O_5 cryogel were calculated using the following equation:

$$D_{Li} = \frac{R^2T^2}{2A^2n^4F^4c^2\sigma^2}$$

where R is the gas constant, T is the absolute temperature, A is the electrode area, n is the number of electrons transferred per molecule during electrochemical reaction, F is Faraday constant, c is molar concentration of Li^+, and σ^2 is the Warburg impedance coefficient. The relationship between real part of impedance and frequency is shown in Fig. S12, and the slope of the fitted line is the Warburg impedance coefficient. The calculated lithium-ion diffusion coefficient of 2D V_2O_5/graphene heterostructure is 2.5×10^{-10} cm^2 s^{-1}, which is much higher than that of V_2O_5 cryogel (5.6×10^{-11} cm^2 s^{-1}).

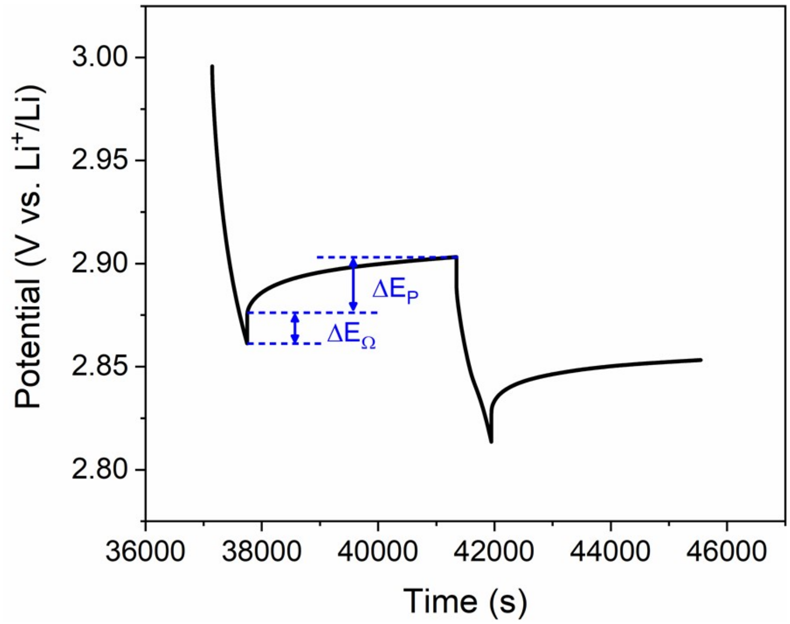

Fig. S13 Typical GITT profile of 2D V_2O_5/graphene heterostructure. ΔE_Ω represents the ohmic *IR* drop; ΔE_p represents the polarization voltage drop induced by charge-transfer impedance and diffusion impedance. The whole overpotential is the sum of ΔE_Ω and ΔE_p.

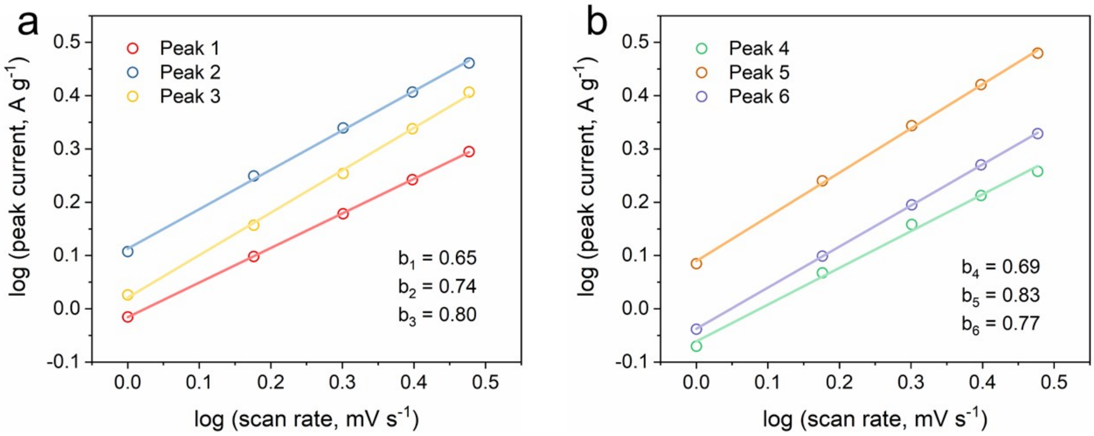

Fig. S14 Linear relationship between log of peak current and log of scan rate for (a) cathodic peaks and (b) anodic peaks in the CV curves of 2D V_2O_5/graphene heterostructure.

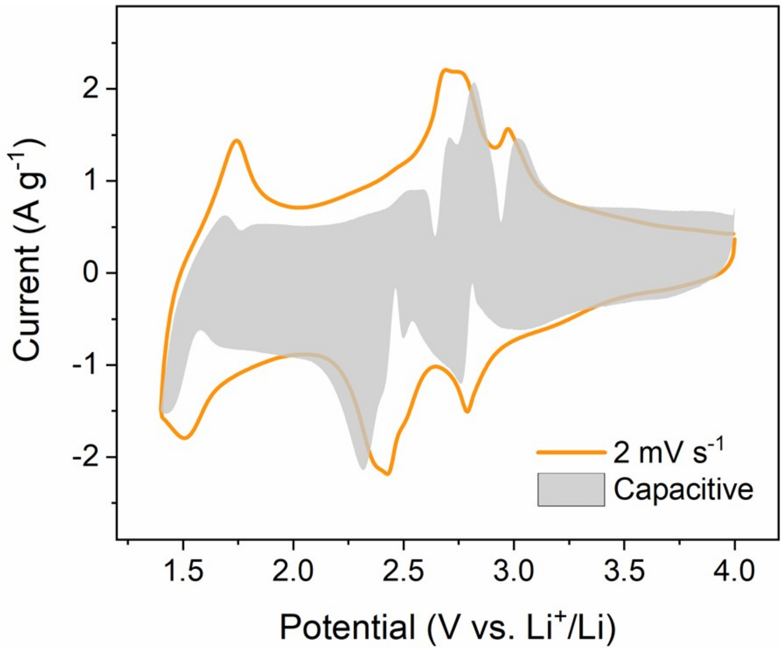

Fig. S15 Capacitive current response (grey) at a scan rate of 2 mV s^{-1}.

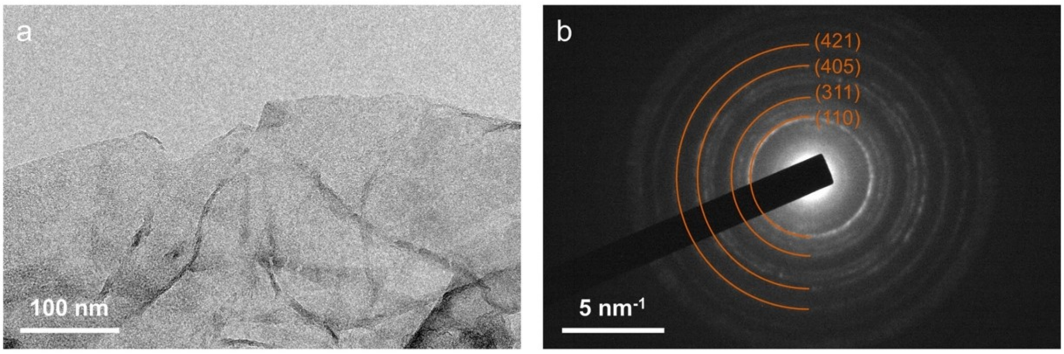

Fig. S16 (a) TEM image and (b) SAED pattern of 2D V_2O_5/graphene heterostructure after 20 cycles.

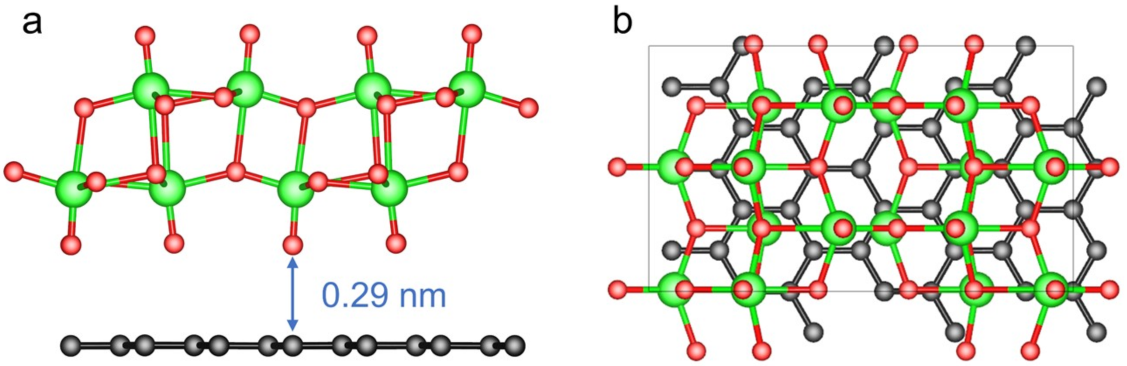

Fig. S17 (a) Side view and (b) top view of the structure model of 2D V_2O_5/graphene heterostructure.

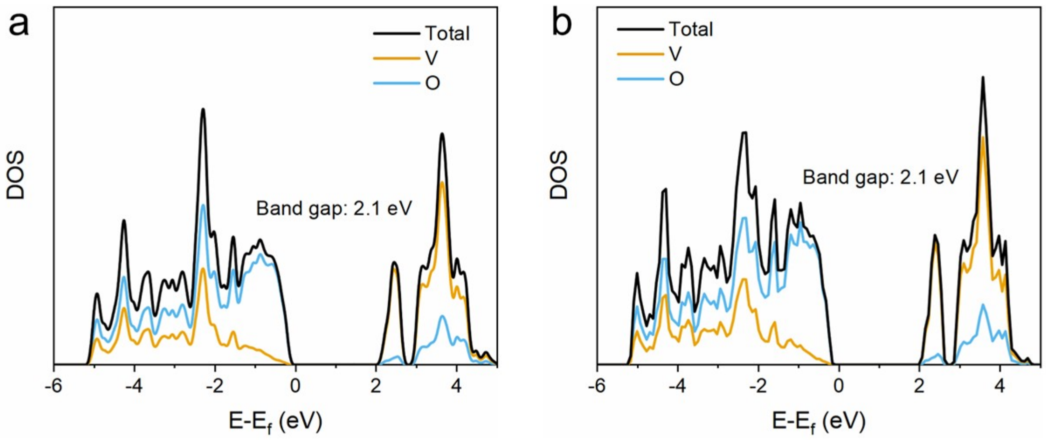

Fig. S18 Density of states of (a) a single layer of bilayered V_2O_5 and (b) bulk bilayered V_2O_5.

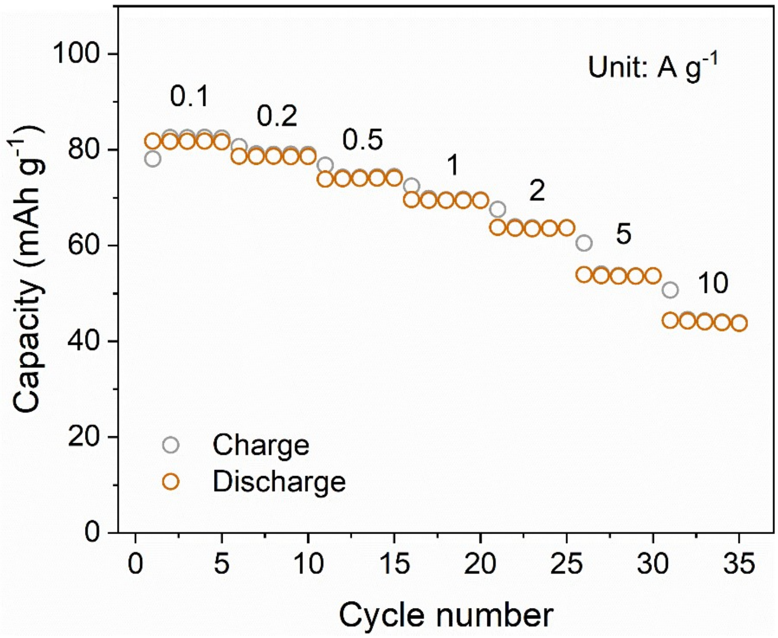

Fig. S19 Rate performance of the symmetric full cell.

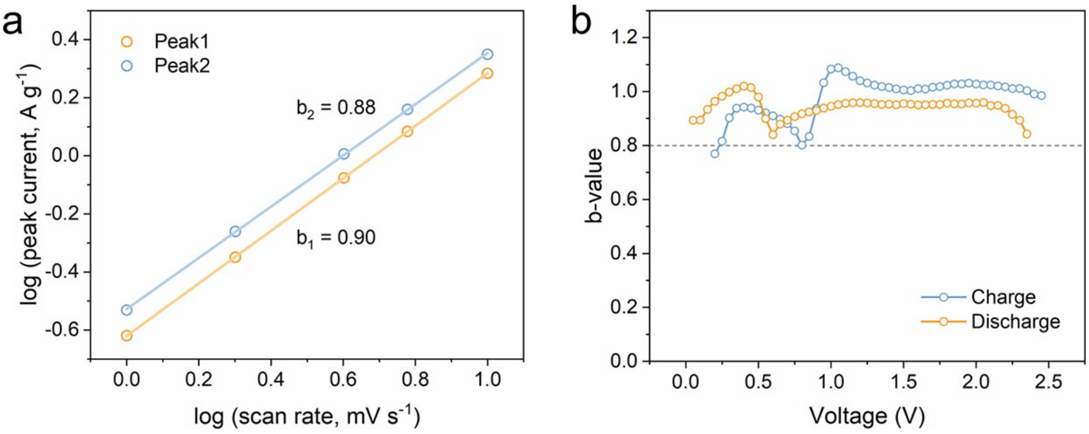

Fig. S20 (a) Linear relationship between log of peak current and log of scan rate for the two peaks in the CV curves of the symmetric full cell. (b) *b* value as a function of voltage for the symmetric full cell.

Table S1 Charge transfer resistances of the symmetric full cell obtained at different charge/discharge states

	Charge			**Discharge**		
Voltage (V)	0.6	1.2	2.4	1	0.4	0
Rct (Ω)	4.6	4.5	4.1	4.2	4.3	4.4

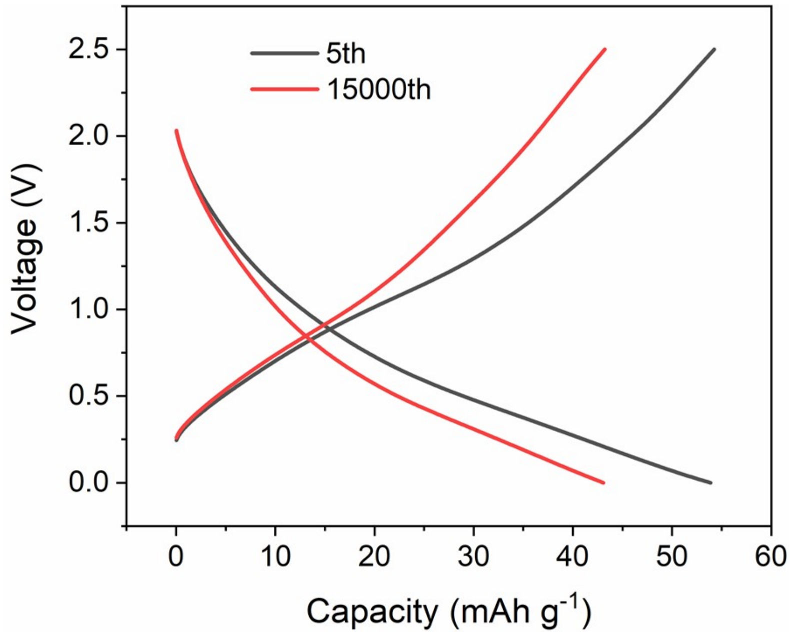

Fig. S21 GCD profiles of the symmetric full cell at the 5th and 15000th cycles.

References

[1] B. Alonso and J. Livage, *J. Solid State Chem.*, 1999, **148**, 16-19.

[2] G. Kresse and J. Furthmuller, *Phys. Rev. B*, 1996, **54**, 11169-11186.

[3] P. E. Blochl, *Physical Review B*, 1994, **50**, 17953-17979.

[4] J. P. Perdew, K. Burke and M. Ernzerhof, *Phys. Rev. Lett.*, 1996, **77**, 3865-3868.

[5] S. Grimme, J. Antony, S. Ehrlich and H. Krieg, *J. Chem. Phys.*, 2010, **132**, 154104.

[6] S. Grimme, S. Ehrlich and L. Goerigk, *J. Comput. Chem.*, 2011, **32**, 1456-1465.

[7] S. L. Dudarev, G. A. Botton, S. Y. Savrasov, C. J. Humphreys and A. P. Sutton, *Phys. Rev. B*, 1998, **57**, 1505-1509.